Research Article | Vol. 26, No. 2 | 22 Jan 2018 | OPTICS EXPRESS 1809
Optics EXPRESS

Unlocking high spatial resolution in neutron imaging through an add-on fibre optics taper

M. Morgano,[1,*] P. Trtik,[1] M. Meyer,[1] E. H. Lehmann,[1] J. Hovind,[1] and M. Strobl[1]

[1]*Laboratory for Neutron Scattering and Imaging, Paul Scherrer Institut, 5232, Villigen, Switzerland*
[*]*manuel.morgano@psi.ch*
http://niag.psi.ch

Abstract: The demand for high resolution neutron imaging has been steadily increasing over the past years. The number of facilities offering cutting edge resolution is however limited, due to (*i*) the design complexity of an optimized device able to reach a resolution in the order of $\approx 10\ \mu$m and (*ii*) limitations in available neutron flux . Here we propose a simple addition, based on a Fibre Optics Taper (FOT), that can be easily attached to an already existing scintillator-camera imaging detector in order to efficiently increase its spatial resolution and hence boost the capability of an instrument into high resolution applications.

OCIS codes: (040.1490) Cameras; (060.2340) Fiber optics components; (110.2970) Image detection systems; (120.4820) Optical systems; (230.0040) Detectors.

References and links

1. M. Strobl, I. Manke, N. Kardjilov, A. Hilger, M. Dawson, and J. Banhart, "Advances in neutron radiography and tomography," Journal of Physics D: Applied Physics **42**, 243001 (2009).
2. E. H. Lehmann, P. Vontobel, E. Deschler-Erb, and M. Soares, "Non-invasive studies of objects from cultural heritage," Nuclear Instruments and Methods in Physics Research Section A: Accelerators, Spectrometers, Detectors and Associated Equipment **542**, 68 – 75 (2005). Proceedings of the Fifth International Topical Meeting on Neutron Radiography.
3. D. Penumadu, *Material Science and Engineering with Neutron Imaging* (Springer US, 2009), pp. 209–227.
4. M. Zarebanadkouki, A. Carminati, A. Kaestner, D. Mannes, M. Morgano, S. Peetermans, E. Lehmann, and P. Trtik, "On-the-fly neutron tomography of water transport into lupine roots," Physics Procedia **69**, 292 – 298 (2015). Proceedings of the 10th World Conference on Neutron Radiography (WCNR-10) Grindelwald, Switzerland October 5âĂŞ10, 2014.
5. A. Kaestner, E. Lehmann, and M. Stampanoni, "Imaging and image processing in porous media research," Adv. Water Resources **31**, 1174 – 1187 (2008). Quantitative links between porous media structures and flow behavior across scales.
6. D. Kramer, J. Zhang, R. Shimoi, E. Lehmann, A. Wokaun, K. Shinohara, and G. G. Scherer, "In situ diagnostic of two-phase flow phenomena in polymer electrolyte fuel cells by neutron imaging," Electrochimica Acta **50**, 2603 – 2614 (2005).
7. N. Kardjilov, I. Manke, M. Strobl, A. Hilger, W. Treimer, M. Meissner, T. Krist, and J. Banhart, "Three-dimensional imaging of magnetic fields with polarized neutrons," Nat. Phys. **4**, 399 (2008).
8. P. Trtik and E. H. Lehmann, "Progress in high-resolution neutron imaging at the paul scherrer institut-the neutron microscope project," J. Phys.: Conf. Series **746**, 012004 (2016).
9. E. Lehmann, G. Frei, G. Kühne, and P. Boillat, "The micro-setup for neutron imaging: A major step forward to improve the spatial resolution," Nuclear Instrum. Methods Phys. Res. Section A **576**, 389–396 (2007).
10. E. Calzada, F. Gruenauer, M. Mühlbauer, B. Schillinger, and M. Schulz, "New design for the antares-ii facility for neutron imaging at frm ii," Nuclear Instrum. Methods Phys. Res. Section A **605**, 50–53 (2009).
11. N. Kardjilov, A. Hilger, I. Manke, M. Strobl, M. Dawson, S. Williams, and J. Banhart, "Neutron tomography instrument conrad at hzb," Nuclear Instrum. Methods Phys. Res. Section A **651**, 47–52 (2011).
12. D. Hussey, D. Jacobson, M. Arif, P. Huffman, R. Williams, and J. Cook, "New neutron imaging facility at the nist," Nuclear Instrum. Methods Phys. Res. Section A **542**, 9–15 (2005).
13. A. Tremsin, J. McPhate, J. Vallerga, O. Siegmund, J. Hull, W. Feller, and E. Lehmann, "Detection efficiency, spatial and timing resolution of thermal and cold neutron counting mcp detectors," Nuclear Instrum. Methods Phys. Res. Section A **604**, 140–143 (2009).
14. D. S. Hussey, J. M. LaManna, E. Baltic, and D. L. Jacobson, "Neutron imaging detector with 2 micrometer spatial resolution based on event reconstruction of neutron capture in gadolinium oxysulfide scintillators," Nuclear Instrum. Methods Phys. Res. Section A **866**, 9 – 12 (2017).

#314745 https://doi.org/10.1364/OE.26.001809
Journal © 2018 Received 6 Dec 2017; revised 10 Jan 2018; accepted 12 Jan 2018; published 17 Jan 2018

Optics EXPRESS

15. A. Faenov, M. Matsubayashi, T. Pikuz, Y. Fukuda, M. Kando, R. Yasuda, H. Iikura, T. Nojima, T. Sakai, M. Shiozawa, R. Kodama, and Y. Kato, "Using lif crystals for high-performance neutron imaging with micron-scale resolution," High Power Laser Sci. Eng. **3**, e27 (2015).
16. P. Trtik and E. H. Lehmann, "Isotopically-enriched gadolinium-157 oxysulfide scintillator screens for the high-resolution neutron imaging," Nuclear Instrum. Methods Phys. Res. Section A **788**, 67–70 (2015).
17. E. Lehmann, P. Vontobel, and L. Wiezel, "Properties of the radiography facility neutra at sinq and its potential for use as european reference facility," Nondestructive Testing Evaluation **16**, 191–202 (2001).
18. A. Kaestner, S. Hartmann, G. Kühne, G. Frei, C. Grünzweig, L. Josic, F. Schmid, and E. Lehmann, "The icon beamline–a facility for cold neutron imaging at sinq," Nuclear Instrum. Methods Phys. Res. Section A **659**, 387–393 (2011).
19. C. Grünzweig, G. Frei, E. Lehmann, G. Kühne, and C. David, "Highly absorbing gadolinium test device to characterize the performance of neutron imaging detector systems," Rev. Sci. Instrum. **78**, 053708 (2007).

1. Introduction

Neutron imaging is a non-destructive investigation technique able to probe the inner structure of bulk objects. Over the years neutron imaging has developed from a qualitative testing technique to a scientific tool with applications in numerous and diverse fields [1], ranging from cultural heritage [2] to engineering [3] and life science [4], from porous media research [5] and liquid phase flow investigation [6] to fundamental physics [7]. The growing field of applications was predominantly a consequence of maturing instrumentation and of the introduction of digital imaging detectors. However, it was also sustained by the ever improving spatial resolution capabilities of digital imaging from originally a few hundreds of micrometers to below 10 μm nowadays [8].

Due to the fact that different applications have different requirements with respect to the size of the field-of-view (FoV) on the one hand and the spatial resolution on the other, state-of-the-art instruments feature a flexible detector set-up with various capabilities in order to efficiently tailor these parameters to the requirements of a specific measurement. For instruments with neutron imaging capabilities at Paul Scherrer Institut (Switzerland), detector systems are available with FoV ranging from 400×400 to 5×5 mm^2 with corresponding best spatial resolution ranging from 200 μm to 5 μm. These systems are correspondingly referred to as *maxi-setup* (resolution $\approx$ 200 μm), *midi-setup* (resolution $\approx$ 100 μm), *micro-setup* [9] (resolution $\approx$ 25 μm) and *Neutron Microscope* [8] (resolution $\approx$ 5 μm).

Despite the growing demand, not many neutron facilities worldwide can provide spatial resolutions < 50 μm due to the aforementioned design complexity of an optimized detection system and limitations to the available neutron flux. Currently these in particular are the ANTARES beamline in Munich (Germany) [10], the CONRAD beamline in Berlin (Germany) [11] and NIF at NIST [12] (USA). All of these facilities utilize the standard approach of optical lens systems to focus (and in some cases zoom) the image produced by a thin scintillator onto the pixelated sensor of a digital camera. A few other approaches for high resolution neutron imaging exist, such as MCP-based detectors [13], post-processing [14], or off-line using LiF crystals [15],.

However, while they might have advantages in a few specific application, none of them is currently surpassing the standard solution in terms of flexibility and adaptability. Therefore here we focus on scintillator and camera-based standard systems for comparison, as they are by far the most common and are those routinely used in our user experiments.

Here we propose and introduce a solution which might be suitable to overcome some of the technological limitations of high-resolution neutron imaging for many more facilities. It is based on the utilization of a magnifying "fibre optic taper (FOT)" coupled with a standard imaging detector setup, readily available at every state-of-the-art facility. Such add-on enables to scale up the spatial resolution straightforwardly while keeping a good light efficiency. This solution also features little technological challenge and requires only a minor additional investment.

Optics EXPRESS

2. Experimental set-up

2.1. Fibre optic taper

A Fibre Optic Taper (FOT) is a device made of small boron glass filaments with gradually increasing diameter. Each of these filaments is coated in order to guide the light inside it without cross-talk among filaments, which are bundled together with others in such a way as to prevent cross-over of filaments, i.e. the filaments preserve their ordered arrangement from one end of the device to the other. The final taper is a truncated-cone shaped solid piece of glass. Such FOTs efficiently transports light from one end to the other, providing in this way a magnification or reduction of an image depending on the direction of use. The FOT used in this work features a length of 11 cm, a diameter of 14 mm on the scintillator side and of 78 mm at the exit of the light, towards the following standard optical and camera system. Its magnification factor, as stated by the manufacturer (Incom, Inc., Massachusetts, USA) equals $6 \pm 0.2\%$. Its constituent fibres have a diameter starting from $\approx 2.5 - 3$ μm and ending at $\approx 15 - 18$ μm, hence limiting the possible spatial resolution to $5 - 6$ μm. Due to the packing of the fibres, it has a dead area of 50%.

Considering the Boron content of the utilized glass fibers, one concern about the use of FOT for neutron imaging might be its stability upon longterm neutron irradiation. However, the neutron flux/absorption estimations suggest that the affected number of nuclei will be low and therefore the possible radiation damage of the FOT is likely to be negligible. In the current experiments, no damage has been hitherto observed.

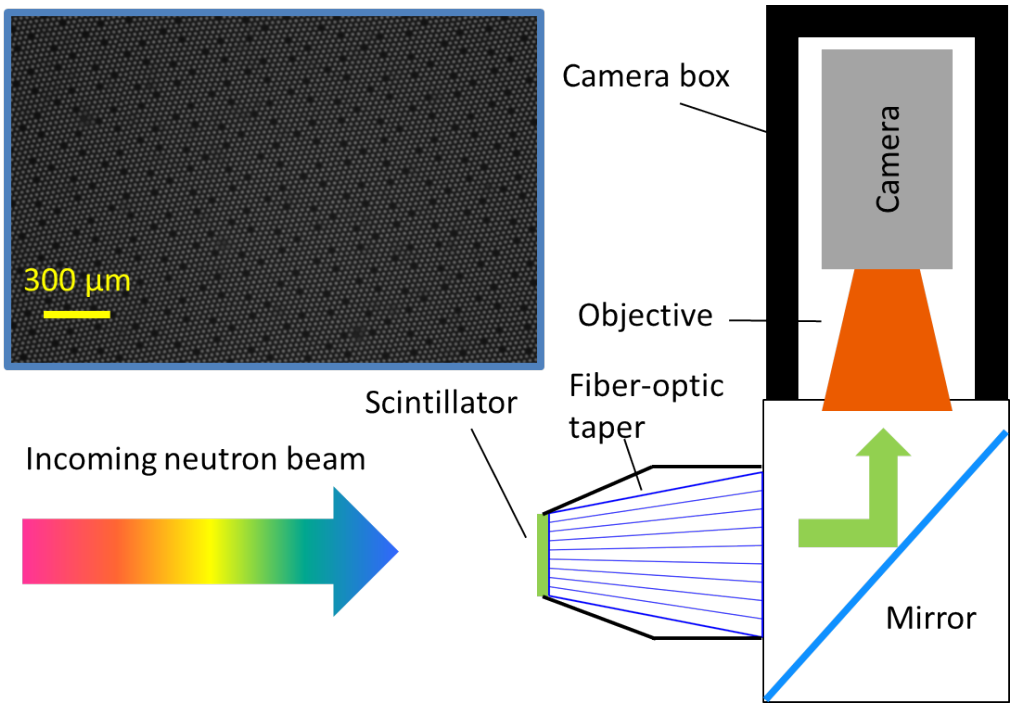

Fig. 1. Schematics of the experimental arrangement. The taper is attached to the camera box in the place where standard scintillators are usually placed. The remaining setup is untouched. In the cut-out on the upper left, an image of the taper obtained with the neutron microscope objective using visible light. The black dots visible in this image are non-light-carrying fibres intentionally embedded in the matrix to suppress cross talk between adjacent fibres. They are too small to be resolved using standard neutron imaging systems.

Optics EXPRESS

2.2. Detector systems

The setup used for the presented experiments was based on the available medium resolution device (*midi-setup*) and consists of a light tight box including a 45 deg optical mirror. Such an arrangement is found at any state-of-the-art facility and is hence a representative system to demonstrate the capability of the taper. A custom designed adapter that tightly fits the FOT to the camera box of the *midi-setup* contains also the front-end interface to the exchangeable neutron scintillator at the small end of the taper (Fig. 1). For the measurements the camera box was equipped with an sCMOS NEO camera from Andor with 2160×2560 pixels. Two different light optics were used with the camera, namely a 50 mm 1:1 lens and a 100 mm 2:1 zoom lens (both from Nikon). The focusing of the camera is conveniently performed using the visible ambient light arriving through the taper when leaving the front side of the taper open, i.e. without having the scintillator installed. This way, a sufficiently high-resolution optics/camera system can, when in focus, resolve the single fibres at the taper exit, which in this case has been used for focusing the system as visible in the cut-out of Fig. 1. After the camera is focused, a suitablei neutron scintillator is placed in direct contact with the small end (entrance) of the FOT and is fixed in a light-tight manner. The scintillators used for these experiments were obtained from RC-Tritec Ltd. (Switzerland), and are standard scintillators used in the operation of the *micro-setup* at the imaging beamlines at PSI. These are Gadox-based binder-stabilized scintillators with a thickness of 10 μm and 20 μm as well as a scintillator for medium resolution imaging (50 μm resolution) consisting of a mixture of ZnS and ^{6}LiF. The latter offers an inherently high light yield. In addition, a ^{157}Gd-enriched Gadox scintillator developed inhouse for highest spatial resolution ([16]) with a thickness of 5 μm was utilized and tested (Table 1).

2.3. Beamlines and test samples

The experiments were performed at the imaging beamlines NEUTRA [17] and ICON [18] at the SINQ neutron source of the PSI. NEUTRA is a thermal neutron instrument with a Maxwellian spectrum with an average wavelength of at 1.5 Å, while ICON, placed viewing a cold source, offers a colder spectrum with an average wavelength of 2.8 Å. ICON in addition offered the opportunity to compare the results achieved with the taper combined with the *midi-setup*, which utilizes standard commercial optics, directly with corresponding results at the same beam conditions achieved with the *micro-setup*, which features a sophisticated custom designed high resolution optics system. Furthermore, ICON measurements offered the opportunity to test the taper configuration with x-rays from an implemented x-ray microfocus tube (L12161-07 from Hamamatsu, Japan).

In order to assess the performance of our configuration (Table 1), we used a Siemens star-resolution pattern [19] which has become an accepted standard in neutron imaging. Figure 2 displays corresponding images where the size of the Gd spokes touching the outer ring is 50 μm and that at the inner ring is 25 μm, allowing direct assessment of the inherent resolution capabilities of our set-ups. For all the measurements, the Siemens star was placed in direct contact with the scintillator screen.

3. Measurements and results

The different combinations of lenses and scintillators led to a variety of different sizes of FoV as well as to different efficiencies and light outputs. Correspondingly different exposure times have been applied in different cases. For each image of the resolution test pattern, corresponding dark-current exposures (images taken with the shutter closed) and open beam images were recorded for background correction and normalization. The main measurement parameters are summarized in Table 1, together with the main results of achieved spatial resolutions.

The obtained images were digitally processed in a standard manner including spot-cleaning,

Optics EXPRESS

background subtraction and normalization.

Table 1. Summary of the results of the measurements with the FOT for all the tested conditions with neutrons. The measurements were all performed with the Andor NEO camera.

#	Beamline	Objective	pixel size	FOV	exposure	OB gray level	OB/pixel area/s	scint. type	scint. thickness	resolution
1	NEUTRA FOT	50 mm	8.3 μm	10×10 mm^2	60 s	7k	1.69	^{6}LiF+ZnS	50 μm	50 μm
2	NEUTRA FOT	50 mm	8.3 μm	10×10 mm^2	120 s	7k	0.85	Gadox	20 μm	25 μm
3	NEUTRA FOT	100 mm	2.6 μm	5.5×6.5 mm^2	300 s	4.4k	2.17	Gadox	20 μm	25 μm
4	NEUTRA FOT	100 mm	2.6 μm	5.5×6.5 mm^2	300 s	2.3k	1.13	Gadox	10 μm	15 μm
5	ICON FOT	50 mm	8.3 μm	10×10 mm^2	90 s	23k	3.71	Gadox	20 μm	22 μm
6	ICON FOT	100 mm	2.6 μm	5.5×6.5 mm^2	300 s	9k	4.44	Gadox	10 μm	16 μm
7	ICON FOT	100 mm	2.6 μm	5.5×6.5 mm^2	300 s	1.7k	0.84	^{157}Gadox	5 μm	11 μm
8	ICON MICRO	taylored	6.5 μm	27×27 mm^2	90 s	3.3k	0.87	Gadox	20 μm	25 μm

3.1. High resolution setup

Utilizing the 50 mm objective in the *midi-setup*, with the taper holder, the visible portion of the large end of the FOT (60 mm wide) occupies a circular region of the sCMOS chip of the diameter of $\approx$ 1200 pixels and images a region of 10 mm wide in diameter. Due to the 6-fold magnification, the resulting effective pixel size is therefore 8.3 μm. This is the same order of magnitude of the effective pixel size as in the *micro-setup*, and hence it enables a straight forward comparison of the *taper* + *midi-setup* system with the *micro-setup*, with its dedicated and elaborated optics system. In order to assess the relative light transport efficiency, the same scintillator and the same exposure time (90 s) were used. For simplicity, we used the available x-ray source for this test. The resulting images are shown in Fig. 2. A first visual inspection suggests a slightly better

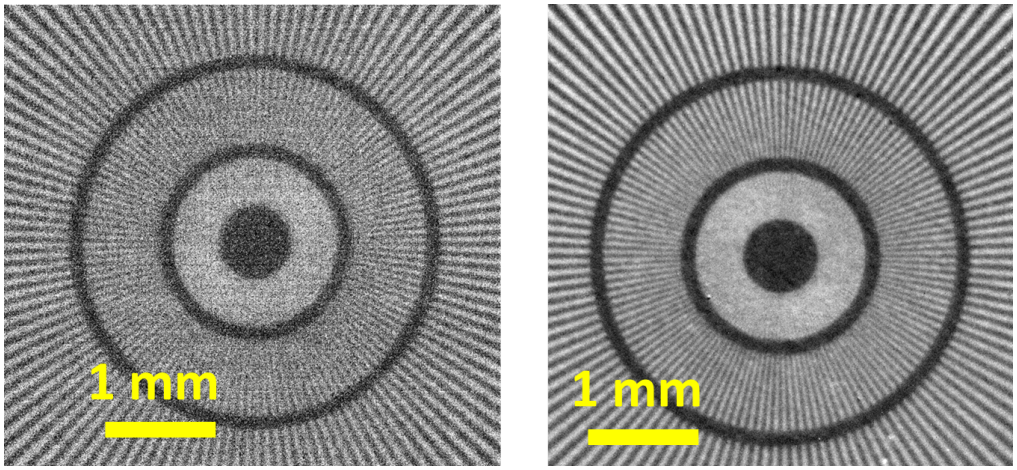

Fig. 2. Comparison between the *micro-setup* (left) and the FOT-setup (right). In both images, the same camera (Andor NEO, Andor, UK) was used. For reference, the size of the spokes at the outer edge of the inner ring of the test pattern is 25 μm.

resolution in the case of the FOT set-up as well as clearly a lower noise level in that case. A rigorous assessment of the resolution by calculating the Modulation Transfer Function (MTF) provides similar results for both, but results are slightly in favor of the FOT with 22 μm versus 25 μm in the case of the *micro-setup*, at 10% modulation. The clear impression with respect to the image noise is unambiguously confirmed by a quantitative inspection of the recorded count rates in the open beam images with both configurations. In the case of the *micro-setup*, the open beam, when corrected for the dark current, has a grey level value (averaged in a wide area of the picture) of 6000, while for the same exposure time and the same averaging area, the FOT setup

Optics EXPRESS

delivers images with 42000 grey levels, meaning that the light transport efficiency of the taper with standard optics is 4.3 higher than the one of the dedicated, high resolution lens system of the *micro-setup* when correctly normalized to the respective different pixel area of the two systems.

More measurements with the 50 mm optics from Nikkon were performed at the NEUTRA beamline. Two different types of scintillator screens were used in these measurements. A ^{6}LiF+ZnS with a thickness of 50 μm and a Gadox based scintillator of 25 μm. The lower efficiency of thin Gadox scintillators in many cases prohibits their use at NEUTRA with its thermal neutron spectrum, which is detected with lower efficiency than cold neutrons. Here, despite the sub-optimal spectrum for the scintillator material and with a particularly thin scintillator for high resolution, the results in Tab. (1) line 1 and 2, confirm that the high efficiency of the FOT enables to acquire high-resolution neutron images, in this case of 50 and 25 μm, respectively. Exposure times required were similar to those needed with the dedicated *micro-setup* at the more intense ICON beamline featuring additionally an advantageous colder spectrum. This again underlines the high efficiency of the system with the FOT, despite the low effort for its realization, which is in strong contrast to the realization of sophisticated optics such as the ones used in the *micro-setup*. An example of these results is provided in Fig. 3, where with a 20 μm-thick Gadox scintillator and an exposure time of 120 s, an open beam image with 7000 grey levels could be recorded in the thermal beam of NEUTRA.

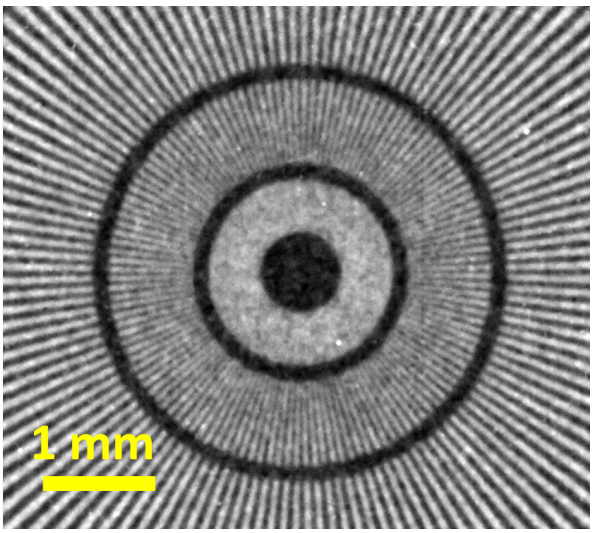

Fig. 3. High resolution neutron image of the test pattern taken at NEUTRA.

The image demonstrates, and the quantification of the achieved spatial resolution clearly implies, that the quality is on par with that obtained at the cold neutron imaging instrument ICON with the dedicated *micro-setup* at higher flux.

3.2. Beyond 25 micron resolution

The intrinsic resolution of the camera system can be improved by employing a 100 mm 2:1 zoom lens which is available for such purpose at the PSI imaging beamlines. With this lens, however only a part of the taper exit side can be imaged and the FOV becomes limited to 5.5×6.5 mm^2 resulting in an effective pixel size of ≈ 2.6 μm. As expected, when using the same 20 μm-thick Gadox scintillator with an increased exposure time of 300 s at the ICON beamline, the use of the 100 mm lens improves the spatial resolution slightly from 25 to 20 μm. The exposure time needs to be increased as a smaller area is now imaged with the same amount of pixels. The limited

Optics EXPRESS

resolution increase underlines the limitation of the resolution by the thickness of the scintillator and its intrinsic blur. Figure 4 highlights the area of the test pattern where the improvement is visible with spokes resolved below 25 micrometer. Visual inspection as well as analyses provide a resolution value of 22 μm. The exposure time at the given experimental condition resulted in an open beam image with 17k grey levels.

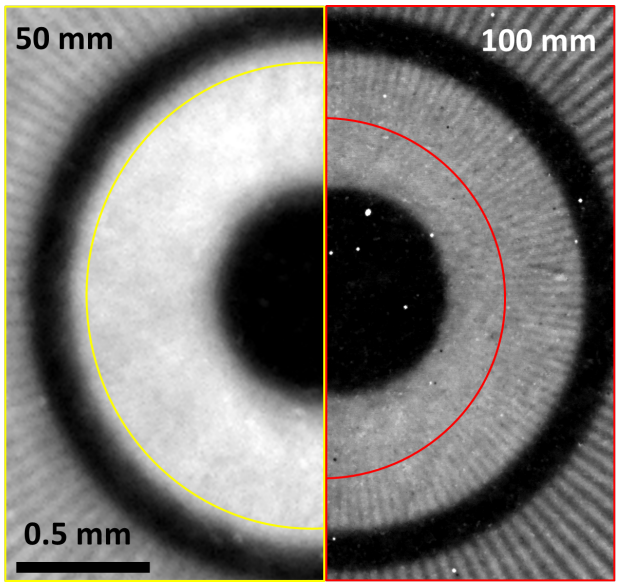

Fig. 4. Comparison between the test patter image taken with the FOT and a 50 mm objective (left) and a 100 mm 2:1 zoom objective (right). All the other parameters of the experimental arrangement remained the same. The slight increase in resolution using the zoom lens is evident, pointing towards the scintillator being the bottleneck for the resolution in this configuration.

Given the small effective pixel size of this setup, it appears that the resolution can be further improved by employing a thinner scintillator. Therefore further measurements were conducted with 10 μm Gadox and 5 μm ^{157}Gd-enriched Gadox based scintillators. The left side of Fig. 5 shows the result with the 10 μm screen with an exposure time of 300 s at ICON resulting in 9k grey levels in the open beam image. A resolution of 16 μm could be achieved in this case.

The 5 μm-thick screen was a special ^{157}Gd-enriched Gadox scintillator [16] in order to improve the efficiency by counteracting the lower thickness chosen for better spatial resolution with the especially high neutron absorption cross section of this Gd isotope. Naturally, the higher neutron absorption leads to higher gamma background, which required particular attention in data acquisition and treatment. Both the image of the patterned object and the open beam were recorded five times for 60 s. For each of the resulting stacks, we projected the median of each pixel to suppress white spots caused by gammas. The resulting filtered images could be processed in the usual way. The result is shown in the right side of Fig. 5. The obtained resolution was close to 11 μm with an Open Beam grey level of 1700k, surpassing the best results achieved so far with the *micro-setup* at PSI.

4. Summary and outlook

It has been demonstrated how the usage of a fibre optic taper as an add-on to existing standard neutron scintillator-camera detectors can enhance the achieved spatial resolution significantly. Despite the simplicity of the addition to standard detectors, the performances surpassed the one

Optics EXPRESS

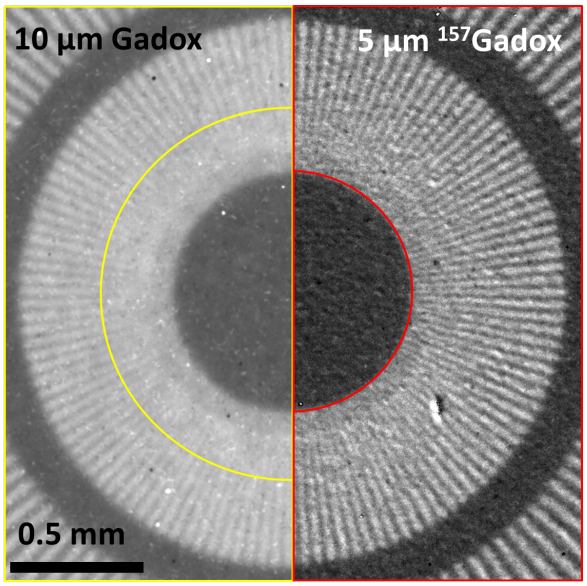

Fig. 5. High resolution neutron image of the test pattern taken at the ICON beamline with a 10 μm-thick Gadox scintillator (left) and a 5 μm-thick ^{157}Gd-enriched Gadox scintillator (right).

of existing high resolution detector devices featuring sophisticated and expensive optics not only in resolution but in particular in efficiency. A 4.3-fold increase in light transport efficiency could be obtained in comparison with an existing dedicated optics, which is a substantial gain and an outstanding achievement in itself, given the flux limitations in high resolution neutron imaging. These gains enabled to perform high resolution imaging beyond 50 μm resolution and down to 15 μm at the thermal beamline NEUTRA at PSI for the first time, due to the relatively short exposure times. Hence, this technique enables highest resolution imaging at thermal instruments even of medium flux neutron sources. At the cold neutron imaging beamline ICON the add-on enabled the resolution of a detector system to be improved from 50 μm down to 15 μm with standard scintillators and lens systems and to close to 10 μm with a specially designed high resolution scintillator based on ^{157}Gd. This simple and inexpensive add-on solution has the potential to improve the spatial resolution capabilities at a number of state-of-the-art neutron imaging facilities worldwide significantly. Furthermore, the results obtained at NEUTRA can be considered pioneering results in thermal neutron imaging as they unlock high resolution imaging on thermal neutron instruments.

Acknowledgments

The authors would like to thank Incom, Inc. USA (in particular Mr. David Benedict) for providing the FOT for testing purposes, Peter Vontobel for support at NEUTRA beamline and Anders Kaestner for support at ICON beamline.